

Particle Ratios within a statistically corrected hadron resonance gas model and EPOS event-generator at AGS, SPS, RHIC and LHC Energies

Mahmoud Hanafy*

Physics Department, Faculty of Science, Benha University, Benha, Egypt

Abdel Nasser Tawfik†

Future University in Egypt (FUE), 11835 New Cairo, Egypt

Muhammad Maher‡

Helwan University, Faculty of Science, Physics Department, Ain Helwan, Egypt

(Dated: January 8, 2024)

We pursue the investigation of the validity of our recently proposed quantum mechanically correlated statistical hadron gas model (HRG) inspired by a Beth-Uhlenbeck corrected form of the equation of state (EoS) to the ideal hadron resonance gas model (IHRG). We calculate the ratios of some particle yields of equal masses, namely $(\bar{p}/p, K^-/K^+, \pi^-/\pi^+, \bar{\Lambda}/\Lambda, \bar{\Sigma}/\Sigma, \bar{\Omega}/\Omega)$, and some particle yield with unequal masses, namely $(p/\pi^+, k^+/\pi^+, k^-/\pi^-, \Lambda/\pi^-, \bar{p}/\pi^-, \Omega/\pi^-)$. We then study the center-of-mass energy variation of these ratios of particle yields obtained by our proposed HRG model. Our model results are then confronted with the corresponding calculations obtained using the ideal hadron resonance gas (IHRG) model, the Cosmic Ray Monte Carlo (CRMC) EPOS 1.99 simulations, as well as the experimental data from AGS, SPS, RHIC, and ALICE. Our proposed HRG model results generally show very close agreement with the experimental data compared with the other models considered. Especially remarkable is the very good matching obtained by our new HRG model with the experimental data of \bar{p}/π^- and p/π^+ , which suggests that our HRG model might be helpful in describing the famous proton anomaly at top RHIC and LHC energies. However, some experimental data of the ratios of hadron pairs of unequal mass and (multi)strange content, like Λ/π^- and Ω/π^- , appear to be quite underestimated by both our HRG model and the IHRG model, which alert further investigation of the suitability of the thermal hadron gas model(s) and thereby motivate the need for further modification.

PACS numbers: 05.50.+q, 21.30.Fe, 05.70.Ce

Keywords: Hadron Resonance Gas correction, Particle Ratios, CRMC, EPOS 1.99, Hadron Interactions, proton anomaly, effective interactions

I. INTRODUCTION

One of the major objectives of the study of ultrarelativistic heavy-ion (HI) collisions is to gain information on the hadron-parton phase diagram, which is characterized by different phases and different types of the phase transitions [1]. The hadronic phase, where stable baryons build up a great part of the Universe and the entire everyday life, is a well known phase. At high temperatures and/or densities, other phases appear. For instance, at temperatures near 150 MeV [2, 3], chiral symmetry restoration and deconfinement transition take place, where quarks and gluons are conjectured to move almost freely within colored phase known as the strongly coupled quark-gluon plasma (sQGP) [4]. At low temperatures but large densities, the hadronic (baryonic) matter forming compact interstellar objects such as neutron stars is indubitably observed in a conventional way. Moreover, gravitational waves from neutron star mergers have recently been detected, as well [5]. At larger densities, extreme interstellar objects such as quark stars are also speculated[6].

Quantum Chromodynamics (QCD), the gauge field theory that describes the strong interactions of colored quarks and gluons and their colorless bound states, has two important intensive state parameters at equilibrium, namely temperature T and baryon chemical potential μ_b . A remarkable world-wide theoretical and experimental effort has been dedicated to the study of strongly interacting matter under extreme condition of temperature and baryon chemical potential. In Lattice Quantum Chromodynamics (LQCD), different orders of chiral and deconfinement transitions have been characterized, especially at low baryon densities.

In high-energy nuclear or HI collisions, the statistical nature of the particle production allows the utilization of the particle multiplicities and ratios, for example, to conduct systematic studies on the thermal properties of the final state. Over the last few decades, huge experimental data at energies covering up four orders of magnitude of GeV are now available. It turns out that various statistical thermal models [7–15] are remarkably successful in explaining the resulting particle yields and their ratios measured in HI collisions. Such a huge data set allowed us to draw the conclusion that the produced particles seem reaffirming the assumption that hadrons are likely stemming from thermal sources at given temperatures and given chemical potentials. It becomes obvious that such a thermal nature is valid, universally, except for a few baryon-to-meson ratios, such as proton-to-pion at top

^{*}Electronic address: mahmoud.nasar@fsc.bu.edu.eg

[†]Electronic address: a.tawfik@fue.edu.eg

[‡]Electronic address: m.maher@science.helwan.edu.eg

RHIC and LHC energies, known as proton anomaly [16].

It was shown that at equilibrium the particle ratios are well explained by two variables; the chemical freezeout temperature (T_{ch}) and the baryon chemical potential (μ_b). In HI collisions, the chemical freezeout stage occurs when the inelastic reactions cease and the number of produced particles becomes fixed. At this stage, the thermal models, such as the ideal hadron resonance gas (IHRG) model, determine the essential characteristics for dense and hot fireball generated in the HI collisions. As a result, the thermal models are utilized as an essential tool connecting the QCD phase diagram with HI experiments [17, 18], in the sense that the measurements, mainly the particle multiplicities are connected to the number density in the thermal models, which in turn are strongly depending on chemical freezeout parameters; T_{ch} , and μ_b . In this way, we use the language of thermodynamics, correlations, fluctuations, etc., in HI collisions [9].

The ideal hadron resonance gas (IHRG) model is customarily used in the lattice QCD calculations as a reference for the hadronic sector [19, 20]. At low temperatures, they are found to be in quite good agreement with the IHRG model calculations [9], although some systematic deviations have been observed, which may be attributed to the existence of additional resonances not taken into account in the IHRG model calculations based on the well established resonances listed by the particle data group [21] and perhaps to the need to extend the model to incorporate hadron interactions.

It is reported in recent literature that the typical IHRG model performance appears to be inadequate to account for all of the evidence that is currently available and projected by recent lattice QCD simulations.[22, 23]. The conjecture to incorporate various types of interactions has been worked out in various studies [24–27]. When comparing the thermodynamics calculated within the thermal model framework with the corresponding data obtained using lattice QCD methods, one has to decide how to incorporate interactions among the hadrons.

Arguments based on the S-matrix approach [28–30] suggest that the (ideal) IHRG model implicitly incorporates attractive interactions between hadrons which leads to the formation of resonances. More realistic hadronic models take into account the contribution of both attractive and repulsive interactions between the component hadrons. Repulsive interactions in the IHRG model had previously been considered in the framework of the relativistic cluster and virial expansions [29], via repulsive mean fields [31, 32], and via excluded volume (EV) corrections [33–38]. In particular, the effects of EV interactions between hadrons on IHRG thermodynamics [39–46], and on the observables of heavy-ion collisions [10, 47–53] has extensively been studied in the literature. Recently, repulsive interactions have received renewed interest in the context of lattice QCD data on fluctuations of conserved charges.

It was shown that large deviations of several fluctuation observables from the IHRG baseline could well be interpreted in terms of repulsive baryon-baryon interactions [53–55].

The dependence of μ_b and T_{ch} on the nucleon-nucleon center-of-mass energies $\sqrt{s_{NN}}$ constructs a boundary of the chemical freezeout diagram which is very close to the QCD phase diagram [56]. The dependence of T_{ch} on μ_b looks similar to that of the various thermodynamic quantities as calculated in the lattice QCD [17, 18], which in turn are reliable quantities, especially at $\mu_b/T \leq 1$, i.e. at $\sqrt{s_{NN}}$ greater than that of top SPS energies. Accordingly, these boundaries remain featured [57], at lower energies, i.e. larger baryon chemical potential, where the QCD-like effective models, such as the IHRG model [9] and the Polyakov linear-sigma model (PLSM) [16, 58] play a major role. The hybrid event-generators such as the Cosmic Ray Monte Carlo (CRMC) [59–68] models are the frameworks. In the present paper, we report the results of our calculations of some particle ratios based on the CRMC EPOS 1.99 simulations, then compare them with the available experimental results, our corresponding calculations based on the ideal hadron gas (IHRG) model, as well as our calculations based on our recently suggested quantum mechanically correlated statistical correction (HRG) to IHRG model [69]. Our quantum-mechanically corrected HRG model is to be motivated in the next section.

In addition to the main goal of this research, namely to further motivate and test our recently suggested statistical correction to the ideal IHRG model [69], the incorporation of CRMC EPOS 1.99 based data in the present work offers some plausible predictions for the future facilities such as the Nuclotron-based Ion Collider facility (NICA), a future facility at the Joint Institute for Nuclear Research (JINR), Dubna-Russia, the Facility for Antiproton and Ion Research (FAIR) at the Gesellschaft für Schwerionenforschung (GSI), Darmstadt-Germany, the J-PARC heavy ion project (J-PARC-HI) at the Japan Proton Accelerator Research Complex (J-PARC) in Tokai, Japan. These and the BES-II program at RHIC are designed to cover the intermediate temperature region of the QCD phase diagram, while both LHC and top RHIC obviously operate at low μ_b or high T_{ch} , i.e. left part of the typical QCD phase-diagram.

The remaining of the present paper is organized as follows: In Section II, we review the detailed formalism of the conventional ideal (uncorrelated) IHRG model, then we develop the HRG model; a non-ideal (correlated) statistical correction to the IHRG model inspired by Beth-Uhlenbeck (BU) quantum theory of non-ideal gases. Finally, we motivate and describe the simulation model, EPOS event generator implemented in this work. The calculations of some particle ratios based on our recently proposed correction are confronted in Section III with our calculations of the corresponding particle ratios using the IHRG model, and the CRMC EPOS 1.99 simulations. In section III, all our

model-based calculations are confronted with a wide range of experimental data of particle ratios. Finally, section IV is devoted to a summary and conclusion.

II. MODEL DESCRIPTION

In the present paper, we implement the particle interaction probability term originally implemented in the expression for the second virial coefficient in the context of motivating a quantum-mechanical model for molecular interactions worked out by Beth and Uhlenbeck in ref. [70, 71]. We inaugurated this project in [69] in an attempt to suggest a statistical correction to the uncorrelated (ideal) IHRG model.

Beth and Uhlenbeck (BU) suggested a connection between the virial coefficients and the probabilities of finding pairs, triples and so on, of particles near each other. In the classical limit, which is usually designated by sufficiently high temperatures and/or low particle densities, it was shown that these probabilities (explicit expressions are to follow later in this section) can be expressed by Boltzmann factors so long as the de Broglie wavelength, which is a common measure of the significance of the quantum non-locality, is small enough compared with the particle spatial extent measured by the so-called particle "diameter" ¹, which is assumed not to be sharply defined. Such a particle diameter can be considered as a measure of the spatial extent within which a particle can undergo hardcore (classical) interactions. Based on a comparison of the original BU model with experimental results, it was concluded that at sufficiently low temperatures for which the thermal de Broglie wave length is comparable with the particle ² diameter, deviations from the classical excluded volume model due quantum effects will be significant [70].

An extension has been made to the original Beth and Uhlenbeck quantum mechanical model of the particle interactions as proposed in ref. [70] by considering the influence of Bose or Fermi statistics in addition to the effect of the inclusion of discrete quantum states for a general interaction potential that is not necessarily central [71]. The expression for the second virial expansion developed in ref. [70] and then extended in ref. [71] was later generalized using the cluster integral to describe particle interactions provided that those particles don't form bound states [28, 29, 72].

More recently, the quantum mechanical BU approach were used to model the repulsive interactions between baryons in a hadron gas [73]. The second virial coefficient or the excluded volume parameter

¹ Here we use the same descriptor originally used by the authors of [70, 71].

² In the original BU model, the particles considered were molecules such as Helium.

was calculated in [73] within the BU approach and found not only to be temperature dependent, but also to differ dramatically from the classical excluded volume (EV) model result. At temperatures $T = 100 - 200$ MeV, the widely used classical EV model [74–76] underestimates the EV parameter for nucleons at a given value of the nucleon hard-core radius (assumed there to be $\simeq 0.3$ fm) by large factors of 3-4. It is thus concluded in [73] that previous studies, which employed the hard-core radii of hadrons as an input into the classical EV model, have to be re-evaluated using the appropriately rescaled quantum mechanical EV parameters.

In what follows of this section, we first introduce the basic formulation of the ideal IHRG model. Then we develop a statistical (HRG) model inspired by BU quantum theory of non-ideal (correlated) gases [71] as a correction to the ideal (uncorrelated) IHRG model. We thereby implement in the formalism of our calculations a modified version of the partition function of the typical ideal IHRG. Moreover, we give a detailed description of the simulation model; the EPOS event generator, considered for comparison with our model.

A. Non-correlated ideal IHRG model

In the framework of bootstrap picture [77–79], an equilibrium thermal model for an interaction free gas has a partition function $Z(T, \mu, V)$ from which the thermodynamics of such a system can be deduced by taking the proper derivatives. In a grand canonical ensemble, the partition function reads [9, 24, 80–83]

$$Z(T, V, \mu) = \text{Tr} \left[\exp \left(\frac{\mu N - H}{T} \right) \right], \quad (1)$$

where H is Hamiltonian combining all relevant degrees of freedom and N is the number of constituents of the statistical ensemble. Eq. (1) can be expressed as a sum over all hadron resonances taken from recent particle data group (PDG) [21] with masses up to 2.5 GeV,

$$\ln Z(T, V, \mu) = \sum_i \ln Z_i(T, V, \mu) = V \sum_i \frac{g_i}{2\pi^2} \int_0^\infty \pm p^2 d\mu \ln \left[1 \pm \lambda_i \exp \left(\frac{-\varepsilon_i(p)}{T} \right) \right], \quad (2)$$

where the pressure can be derived as $T \partial \ln Z(T, V, \mu) / \partial V$, \pm stands for fermions and bosons, respectively. $\varepsilon_i = (p^2 + m_i^2)^{1/2}$ is the dispersion relation, g_i is the spin-isospin degeneracy factor, and λ_i is the fugacity factor of the i -th particle [9],

$$\lambda_i(T, \mu) = \exp \left(\frac{B_i \mu_b + S_i \mu_s + Q_i \mu_q}{T} \right), \quad (3)$$

where $B_i(\mu_b)$, $S_i(\mu_S)$, and $Q_i(\mu_Q)$ are baryon, strangeness, and electric charge quantum numbers (their corresponding chemical potentials) of the i -th hadron, respectively. From phenomenological point of view, the baryon chemical potential μ_b - along the chemical freezeout boundary, where the production of particles is conjectured to cease - can be related to the nucleon-nucleon center-of-mass energy $\sqrt{s_{NN}}$ using the following parameterization [84]

$$\mu_b = \frac{a}{1 + b\sqrt{s_{NN}}}, \quad (4)$$

where $a = 1.245 \pm 0.049$ GeV and $b = 0.244 \pm 0.028$ GeV $^{-1}$. In addition to pressure, the number and energy density, respectively, and likewise the entropy density and other thermodynamics can straightforwardly be derived from the partition function by taking the proper derivatives

$$n_i(T, \mu) = \sum_i \frac{g_i}{2\pi^2} \int_0^\infty p^2 dp \frac{1}{\exp\left[\frac{\mu_i - \varepsilon_i(p)}{T}\right] \pm 1}, \quad (5)$$

$$\rho_i(T, \mu) = \sum_i \frac{g_i}{2\pi^2} \int_0^\infty p^2 dp \frac{-\varepsilon_i(p) \pm \mu_i}{\exp\left[\frac{\mu_i - \varepsilon_i(p)}{T}\right] \pm 1}. \quad (6)$$

It should be noticed that both T and $\mu = B_i\mu_b + S_i\mu_S + \dots$ are related to each other and to $\sqrt{s_{NN}}$ [9]. As an overall thermal equilibrium is assumed, μ_S is taken as a dependent variable to be estimated due to the strangeness conservation, i.e. at given T and μ_b , the value assigned to μ_S is the one assuring $\langle n_S \rangle - \langle n_{\bar{S}} \rangle = 0$. Only then, μ_S is combined with T and μ_b in determining the thermodynamics, such as the particle number, energy, entropy, etc. The chemical potentials related to other quantum charges, such as the electric charge and the third-component of isospin, etc. can also be determined as functions of T , μ_b , and μ_S and each of them must fulfill the corresponding conservation laws.

B. Quantum-statistically correlated HRG model

As informally introduced in the previous section, for a quantum gas of fermions and bosons with mass m_i and correlation (interaction) distance r , at temperature T and vanishing μ_b , a two-particle interaction probability of the form

$$1 \pm \exp(-4\pi^2 m_i T r^2) \quad (7)$$

was first introduced by Beth and Uhlenbeck [71] in an attempt to model the interactions of a quantum gas of particles assuming a general potential and neglecting the possibility for bound states formation. The Boltzmann-like term, $\exp(-4\pi^2 m_i T r^2)$, remains in effect even for an ideal gas, which is a typical approximation at sufficiently high temperatures. The \pm sign expresses the apparent attraction

(repulsion) between bosons (fermions) due to change of statistics. Inspired by such a correction, we introduce a correction to the probability term in the expression for the the ideal hadron gas partition function given in Eq. (1). We propose a new probability term of the form

$$1 \pm \lambda_i \exp\left(\frac{-\varepsilon_i(p)}{T}\right) [1 \pm \exp(-4\pi^2 m_i T r^2)]. \quad (8)$$

This corrected probability function obviously incorporates interactions in the the hadron resonance gas in the sense of BU quantum correlations [71] with r being the correlation (interaction) length between any two hadrons at equilibrium temperature T . Based on our proposed corrected probability function, we modify the non-correlated IHRG partition function $Z(T, \mu, V)$ to have the following form

$$\ln Z(T, V, \mu) = \sum_i V \frac{g_i}{2\pi^2} \int_0^\infty \pm p^2 d\ln \left[\pm \lambda_i \exp\left(\frac{-\varepsilon_i(p)}{T}\right) \right] [1 \pm \exp(4\pi m_i T r^2)], \quad (9)$$

which apparently sums over all hadron resonances following the same recipe described in motivating Eq. (2) for the case of non-correlated IHRG. The thermodynamics of the correlated HRG model can thus be calculated by taking the proper derivatives of $\ln Z$ as explicitly stated in the corresponding non-correlated IHRG case discussed above.

C. Cosmic Ray Monte Carlo (CRMC) model

As discussed, the hybrid event generator, Cosmic Ray Monte Carlo (CRMC EPOS_{lh}c), is used in generating different particle ratios for various hadrons, at energies spanning between $\sqrt{s_{NN}} = 3$ and 2760 GeV. The EPOS_{lh}c event generator results are then confronted with the available experimental results and finally compared to our quantum-mechanically inspired statistically corrected hadron resonance gas model (HRG) calculations based on Eq. (9) .

The interface of CRMC is used for the different cosmic ray monte-carlo models for different effective quantum chrmodynamic (QCD) theories and various experiments as NA61, ATLAS, CMS, LHCb, and the Pierre Auger observatory for ultra high-energy cosmic rays, etc. It features a variety of interactions based on the EPOS_{lh}c/1.99 model, which is similar to the Gribov-Regge model. CRMC presents a comprehensive background description that takes into account the diffraction that results. Also, its interface can access the output from several heavy-ion collision event generators, and can be connected to models of various spectrum, such as, EPOS 1.99/lhc [67, 68], qgsjetII [61–63], qgsjet01 [59, 60], and sibyll [64–66]. SIBYLL2.3 and QGSJET01 are used at low energies. QGSJETII, v03 and v04, and EPOS lh/1.99 are the effective models that can be incorporated at the ultra-relativistic high energies.

In the present work, we used the EPOS_{lhc} event generator which has different parameters for the essential observables in high-energy heavy-ion collisions and their phenomenological assumptions. These can be changed based on the considered theoretical and experimental postulates. It was reported that EPOS_{lhc} is capable of providing a realistic description for heavy-ion collisions based on the data collected by various experiments and other event generators [67, 68].

EPOS_{lhc} was designed for cosmic ray air showers, but it could also be used for pp- and AA-collisions at SPS, RHIC, and LHC energies. Moreover, EPOS_{lhc} applies simpler treatments for heavy-ion collisions near the end of their evolutions, allowing it to be used for minimal bias in hadron interactions in nuclear collisions [85]. EPOS_{lhc} is considered as a parton model with several parton-parton interactions which lead to different parton ladders. It gives good estimates for particle production, multiple scattering of partons, cross-section evaluations, shadowing and screening through splitting, and different integrated effects of hot and dense matter.

In the present work, we used the EPOS_{lhc} event generator, at energies spanning between 3 and 2760 GeV for a set of at least 100,000 events for each energy. We have calculated the particle ratios for some particle yields of equal masses, namely $(\bar{p}/p, K^-/K^+, \pi^-/\pi^+, \bar{\Lambda}/\Lambda, \bar{\Sigma}/\Sigma, \bar{\Omega}/\Omega)$, and some particle yields with unequal masses, namely $(p/\pi^+, k^+/\pi^+, k^-/\pi^-, \Lambda/\pi^-, \bar{p}/\pi^-, \Omega/\pi^-)$, in a wide rapidity window, namely $-6 < y < 6$. We calculate the particle ratios for the different hadron species examined in the interest of further checking the validity of the hybrid EPOS_{lhc} event generator, which is expected to provide more insight on aspects of possible enhancement of such event generator that support the quest for obtaining novel input that might be relevant to future experimental facilities such as NICA and FAIR.

III. RESULTS AND DISCUSSION

In the figures below, we confront the data of the particle ratios calculated using our quantum-mechanically inspired statistically corrected hadron resonance gas model (HRG) based on Eq. (9) (black solid curves) with our calculations of the same particle ratios using the ideal hadron resonance gas model (IHRG) based on Eq. (2) (red dashed curves), with our corresponding calculations based on CRMC EPOS 1.99 simulations (blue stars), and finally with the corresponding experimental data (different symbols) characterizing the results measured at STAR BES-I [86] and partially at the Alternating Gradient Synchrotron (AGS) [10], the Superproton Synchrotron (SPS) [8], NA49 [87–89], NA44 [87–91], NA57 [92], and PHENIX [93]. A great part of this range of the beam energy shall

be accessed by NICA and FAIR future facilities [94, 95] in the temperature range $T \in [130, 200]$ MeV]. These temperatures are rather typical for the phenomenological applications in the context of heavy-ion collisions and QCD equation-of-state. In all our calculations based on our new HRG model, we set the quantum-mechanical correlation length (parameter) to the optimal value $r = 0.85$ fm.

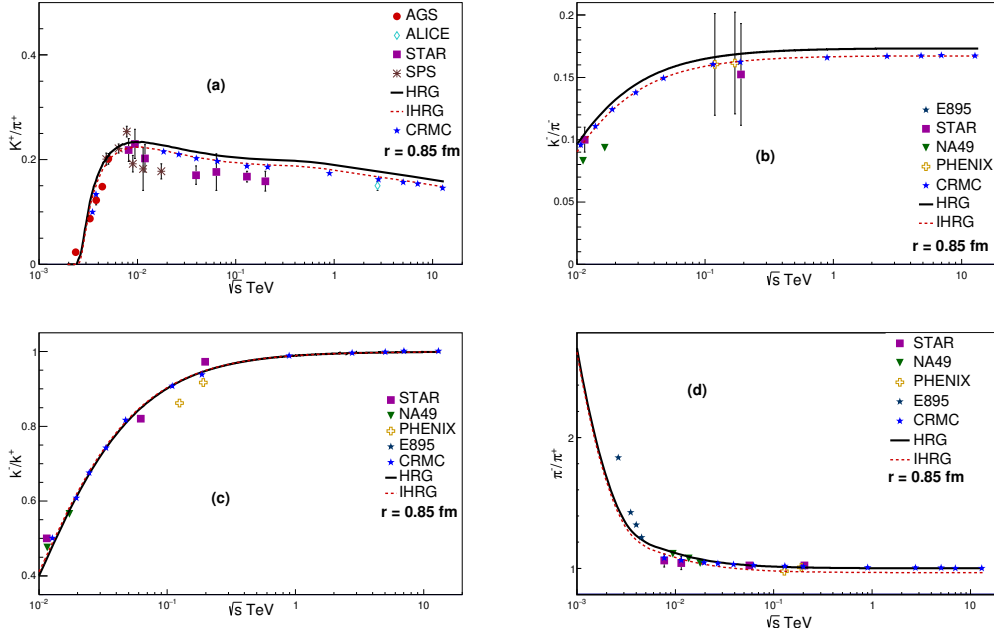


Fig. 1: Variation of the strange meson to non-strange meson ratios k^+/π^+ (a), k^-/π^- (b), antikaon-to-kaon ratio k^-/k^+ (c), and antipion-to-pion ratio π^-/π^+ (d) with respect to center-of-mass energy $\sqrt{s_{\text{NN}}}$. Black solid curve, red dashed curve, and blue stars show the predictions of our new (HRG) model (Eq. 9), the ideal IHRG model (Eq. 2), and CRMC EPOS 1.99 simulations [67, 68], respectively. The corresponding experimental data are represented by different symbols [8, 10, 86, 87, 87, 88, 88, 89, 89–93, 96].

In Figs. 1, we show the center-of-mass energy dependence of the ratio of strange meson to non-strange meson such as k^+/π^+ (a), K^-/π^- (b), and the ratio of antimeson-to-meson such as k^-/k^+ (c), and π^-/π^+ calculated using our new HRG model defined in Eq.9 (Black solid curve), the ideal IHRG model defined in Eq.2 (red dashed curve), and CRMC EPOS 1.99 simulations (blue stars) [67, 68]. The corresponding experimental data of the respective particle ratios used in the comparison are represented by different symbols [8, 10, 86, 87, 87, 88, 88, 89, 89–93, 96].

Like all other types of hadron thermal models, our new quantum-mechanically inspired; statistically corrected HRG model (red dashed curve) slightly overestimates the experimental k^+/π^+ data represented by different symbols in (Fig. 1a) as of about $\sqrt{s_{\text{NN}}} = 3$ GeV. However, our new HRG model (red dashed curve) is slightly closer to fit the experimental data compared with the ideal HRG

model (Black solid curve). Remarkable enough, our new IHRG model (red dashed curve), and also the HRG model (black solid curve), seem to well-reproduce the famous peak near $\sqrt{s_{\text{NN}}} = 10$ GeV in the k^+/π^+ ratio profile (Fig. 1a). Compared to the experimental data, our new IHRG model's calculations as well as the ideal HRG model's calculations for the k^+/π^+ ratio looks much broader at the peak. Starting from the peak, our IHRG model offers the best fit for the available experimental data, especially in the high $\sqrt{s_{\text{NN}}}$ limit where our model fits very closely the 2.76 TeV ALICE measurement [96] of the k^+/π^+ ratio. On the other hand, our CRMC EPOS 1.99 simulations (blue stars) for the k^+/π^+ data are strongly suppressed and obviously doesn't even reproduce the famous peak in k^+/π^+ experimental data, but it catches up with our IHRG model and with the ideal HRG model to closely fit the experimental data as of about $\sqrt{s_{\text{NN}}} = 100$ GeV up to the very high $\sqrt{s_{\text{NN}}}$ limit (~ 10 TeV).

For the k^-/π^- experimental data (Fig. 1b), our new IHRG model (red dashed curve) is generally in very good agreement with the experimental data. It's even slightly better fitting the experimental data than the ideal HRG model (Black solid curve). On the other hand, our CRMC EPOS 1.99 simulations for the k^-/π^- experimental data seem to well-reproduce the steady increase feature in the k^-/π^- ratio (Fig. 1b) but with a significant suppression all over the energy range covered in the present study. This suppression in the CRMC EPOS 1.99 simulations decreases significantly and consistently in the TeV scale.

The variation of the the ratio k^-/k^+ with $\sqrt{s_{\text{NN}}}$ is shown in fig. 1c. Our new IHRG model prediction for the k^-/k^+ profile (red dashed curve) is almost indistinguishable from the prediction of the ideal HRG model (black solid curve). For k^-/k^+ , all featured experimental data show very good agreement with our IHRG model as well as the ideal HRG model. Only the lower energy PHENIX measurement [93] near $\sqrt{s_{\text{NN}}} = 100$ GeV is quiet overestimated by all thermal models considered in this research. Our CRMC EPOS 1.99 simulations for the k^-/k^+ ratio seem to reproduce the monotonic increase feature of the k^-/k^+ experimental data quite well up to the very high energy limit (~ 10 TeV). In the low energy limit up to about $\sqrt{s_{\text{NN}}} = 30$ GeV, CRMC EPOS 1.99 simulations seem to be very well compatible with the data of the k^-/k^+ ratio produced by both the thermal models and the available experimental data. The same feature is observed in the high energy limit from about $\sqrt{s_{\text{NN}}} = 3$ TeV. Between the previous two extreme limits in the intermediate energy regime, our CRMC simulations doesn't fit well with neither the experimental nor the thermal model data.

The variation of the the ratio π^-/π^+ with $\sqrt{s_{\text{NN}}}$ is shown in fig. 1d. For π^-/π^+ , all the featured experimental data show very good agreement with our IHRG model (red dashed curve) as well as with the ideal HRG model (black solid curve) except for the lower energy E895 measurement data $\sqrt{s_{\text{NN}}} \simeq$

2 GeV [97], which are quiet underestimated by all thermal models considered in the present research. Our CRMC simulations data seem to agree well with the considered π^-/π^+ experimental data as well as with the featured thermal models starting from about 10 GeV all the way to (~ 10 TeV).

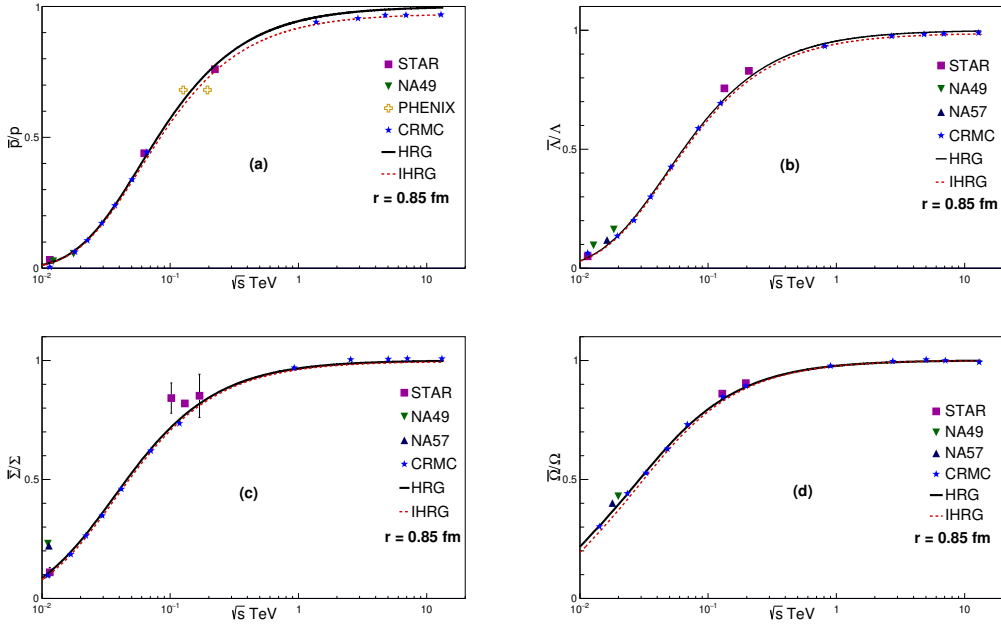


Fig. 2: Variations of the antibaryon-to-baryon ratios such as \bar{p}/p (a), $\bar{\Lambda}/\Lambda$ (b), $\bar{\Sigma}/\Sigma$ (c), and $\bar{\Omega}/\Omega$ (d) with respect to center-of-mass energy $\sqrt{s_{\text{NN}}}$. red dashed curve, Black solid curve, and blue stars (curve) show the predictions of our new IHRG model (Eq. 9), ideal HRG model (Eq. 2), and CRMC EPOS 1.99 [67, 68], respectively. The corresponding experimental points are represented by different symbols [8, 10, 86, 87, 87, 88, 88, 89, 89–93, 96, 98]

In Figure 2, we show the center-of-mass energy dependence of the antibaryon-to-baryon ratios such as \bar{p}/p (a), $\bar{\Lambda}/\Lambda$ (b), $\bar{\Sigma}/\Sigma$ (c), and $\bar{\Omega}/\Omega$ (d) calculated using our new HRG model defined in Eq. 9 (Black solid curve), the ideal IHRG model defined in Eq. 2 (red dashed curve), and CRMC EPOS 1.99 simulations (blue stars curve) [67, 68]. The corresponding experimental data of the respective particle ratios used in the present study are represented by different symbols [8, 10, 86, 87, 87, 88, 88, 89, 89–93, 96, 98].

For the \bar{p}/p ratio (Fig. 2a), It's quite obvious that our new (HRG) model as well as the ideal IHRG model provide a very good agreement with experimental data up to the 200 GeV RHIC data, which is the experimental point with highest energy available. On the contrary, our CRMC simulations seem to severely underestimate the experimental data especially for $20 \text{ GeV} \lesssim \sqrt{s_{\text{NN}}} \lesssim 200 \text{ GeV}$. Up to

about $\sqrt{s_{\text{NN}}} \simeq 200$ GeV, the \bar{p}/p ratio calculated by both our new HRG model and the ideal IHRG model are almost indistinguishable.

On the other hand, the profiles of the ratios $\bar{\Lambda}/\Lambda$ (Fig. 2b) and $\bar{\Sigma}/\Sigma$ (Fig. 2c) shares almost all the important features outlined in discussing the features of the \bar{p}/p ratio (Fig. 2a) except for the obvious fact that the experimental NA49 data at low energies ($\simeq 10$ GeV) seem to be generally underestimated by our thermal model calculations compared with the profile of \bar{p}/p ratio (Fig. 2a).

Our CRMC EPOS 1.99 simulations seem to severely underestimate the experimental data for the whole energy range in the $\bar{\Lambda}/\Lambda$ profile (Fig. 2b), while the same occurs for the $\bar{\Sigma}/\Sigma$ profile (Fig. 2c) except for the very high energy limit ($\sqrt{s_{\text{NN}}} \gtrsim 1$ TeV) where CRMC EPOS 1.99 simulations obviously overestimate the thermal model calculations for the $\bar{\Sigma}/\Sigma$ ratio. Unfortunately, as far as we know, no relevant experimental data are available in this regime.

In Figure 2d, the profile of the ratio $\bar{\Omega}/\Omega$ based on the thermal model calculations, not only underestimates the experimental data at low energies ($\simeq 10$ GeV) but also at the medium energies near ($\simeq 200$ GeV). Here our CRMC EPOS 1.99 simulations seem to overestimate the thermal model calculations in the low energy regime, while it underestimates the experimental data near the 200 GeV RHIC data. Moreover, our (HRG) model calculations (Black solid curve) for this ratio is almost identical to the ideal IHRG model calculations (red dashed curve).

In Figure 3, we show the center-of-mass energy dependence of the antibaryon-to-antimeson ratios such as \bar{p}/π^- (a), baryon-to-meson ratios such as p/π^+ (b), and baryon-to-antimeson ratios such as Λ/π^- (c) and Ω/π^- (d) with respect to center-of-mass energy $\sqrt{s_{\text{NN}}}$ calculated using our new HRG model defined in Eq. 9 (black solid curve), the ideal IHRG model defined in Eq. 2 (red dashed curve), and CRMC EPOS 1.99 simulations (blue stars) [67, 68]. The corresponding experimental data of the respective particle ratios used in the present study are represented by different symbols [8, 10, 86, 87, 87, 88, 88, 89, 89–93, 96, 98].

For the \bar{p}/π^- ratio (Fig. 3a), it's quite obvious that our new (HRG) model provides a very good agreement with the STAR experimental data points available up to 200 GeV, while the ideal IHRG model seems to consistently underestimate the experimental data except at very low energies where all thermal model predictions almost coincide with the lowest energy STAR data. Very much like the IHRG data, the CRMC EPOS 1.99 simulations seem to severely underestimate the experimental data especially at high RHIC energies near 200 GeV all the way to the high energy limit ($\lesssim 10$ TeV).

The ratio p/π^+ (Fig. 3b) shares almost all the important features outlined in discussing the features of the \bar{p}/π^- ratio (Fig. 3a) except that in this case the calculations based on our new HRG model are

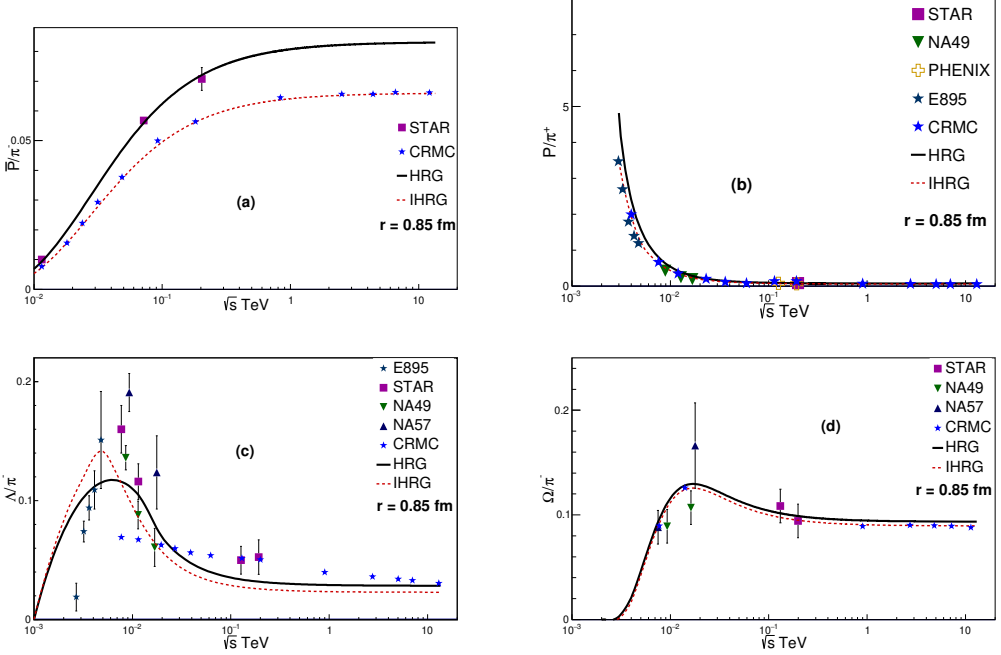


Fig. 3: Variations of the antibaryon-to-antimeson ratios such as \bar{p}/π^- (a), and baryon-to-meson ratios such as p/π^+ (b), Λ/π^- (c), and Ω/π^- (d) with respect to center-of-mass energy $\sqrt{s_{\text{NN}}}$. Black solid curve, red dashed curve, and blue stars show the predictions of our new HRG model (Eq. 9), ideal IHRG model (Eq. 2), and CRMC EPOS 1.99 simulations [67, 68], respectively. The corresponding experimental data are represented by different symbols [8, 10, 86, 87, 87, 88, 88, 89, 89–93, 96, 98]

only slightly better than the corresponding ideal HRG model calculations up to high RHIC energies near 200 GeV.

In Fig. 3c and Fig. 3d, our new IHRG model calculations and the ideal HRG model calculations clearly reproduce the Λ/π^- (Fig. 3c) and Ω/π^- (Fig. 3d) main features of the experimental profiles, especially the peaks near $\sqrt{s_{\text{NN}}} \simeq 2$ GeV in the Λ/π^- profile and near $\sqrt{s_{\text{NN}}} \simeq 20$ GeV in the Ω/π^- profile. Our IHRG model calculations offers a very good prediction of position and the shape of the peak of Λ/π^- ratio profile (Fig. 3c). The sharpness and the height of our model prediction for the peak of Λ/π^- ratio is obviously better than that of the ideal HRG model. For the Ω/π^- profile (Fig. 3d), our new HRG model and the ideal IHRG model are almost equivalently as good in predicting the shape and the position of the peak near about $\sqrt{s_{\text{NN}}} \simeq 20$ GeV. However, the calculations based on our new HRG model and the ideal IHRG model seem to underestimate the height of the Λ/π^- and Ω/π^- peaks. Finally our CRMC EPOS 1.99 simulations doesn't seem to reproduce the Λ/π^- peak at all, while it produces Ω/π^- peak but with a significantly exaggerated height.

IV. SUMMARY AND CONCLUSION

We confronted the data of the particle ratios with respect to center-of-mass energy $\sqrt{s_{\text{NN}}}$ calculated using our new quantum-mechanically inspired and statistically corrected hadron resonance gas model (HRG) based on Eq. (9) with our corresponding calculations of particle ratios using the ideal hadron resonance gas model (IHRG) based on Eq. (2), our corresponding calculations using CRMC EPOS 1.99 simulations, and finally with the corresponding experimental data characterizing the particle yield data measured at STAR BES-I [86] and partially measured at the Alternating Gradient Synchrotron (AGS) [10], the Superproton Synchrotron (SPS) [8] energies, NA49 [87–89], NA44 [87–91], NA57 [92], and finally PHENIX [93]. A major part of this range of the beam energy is expected to be accessed by NICA and FAIR future facilities [94, 95] in the temperature range $T \in [130, 200 \text{ MeV}]$. These temperatures are typical for many phenomenological applications in the domain of heavy-ion collisions and QCD equation-of-state research. It's important here to pay the reader's attention that we have also confronted our new HRG model with with lattice data in a former study [69].

We generally observe a very good agreement between our new HRG model results and the corresponding experimental data. Our new HRG model particularly shows excellent agreement with data of k^-/k^+ , $\bar{\Lambda}/\Lambda$, $\bar{\Sigma}/\Sigma$, $\bar{\Omega}/\Omega$, Ω/π^- , and π^-/π^+ . For the remaining particle ratios, we observe a less agreement between our new HRG model results and the corresponding experimental data. Moreover, it's especially remarkable that our new HRG model exhibits a very good agreement with the pair \bar{p}/π^- and p/π^+ , which suggests that our new HRG model might be helpful in describing and thereby resolving the famous proton anomaly problem at top RHIC and LHC energies [16]. This mandates further investigation to confirm.

Although the ideal IHRG model also exhibits generally a quite good agreement with the corresponding experimental data, we still need a new model that incorporates repulsive interactions between hadrons, which is a major merit in our new HRG model.

In conclusion, the results presented in the present paper supports the claim that our new quantum-mechanically correlated, and statistically corrected HRG model is quite successful in explaining the particle ratios of various particles after chemical freeze-out.

V. REFERENCES

- [1] T. Banks and A. Ukawa, Nuclear Physics B **225**, 145 (1983).
- [2] A. N. Tawfik, M. Maher, A. El-Kateb, and S. Abdelaziz, Advances in High Energy Physics **2020** (2020).
- [3] H.-T. Ding et al., Physical review letters **123**, 062002 (2019).
- [4] E. Shuryak, Reviews of Modern Physics **89**, 035001 (2017).
- [5] B. P. Abbott et al., Phys. Rev. Lett. **119**, 161101 (2017).
- [6] E. S. Fraga, R. D. Pisarski, and J. Schaffner-Bielich, Physical Review D **63**, 121702 (2001).
- [7] A. Andronic, P. Braun-Munzinger, and J. Stachel, Nucl. Phys. A **772**, 167 (2006).
- [8] P. Braun-Munzinger, J. Stachel, J. Wessels, and N. Xu, Physics Letters B **365**, 1 (1996).
- [9] A. N. Tawfik, Int. J. Mod. Phys. A **29**, 1430021 (2014).
- [10] P. Braun-Munzinger, I. Heppe, and J. Stachel, Physics Letters B **465**, 15 (1999).
- [11] J. Cleymans and H. Satz, Zeitschrift für Physik C Particles and Fields **57**, 135 (1993).
- [12] S. Tiwari and C. Singh, Advances in High Energy Physics **2013** (2013).
- [13] J. Rafelski and J. Letessier, Physical review letters **85**, 4695 (2000).
- [14] F. Becattini, J. Cleymans, A. Keränen, E. Suhonen, and K. Redlich, Physical Review C **64**, 024901 (2001).
- [15] J. Cleymans, D. Elliott, A. Keränen, and E. Suhonen, Physical Review C **57**, 3319 (1998).
- [16] A. N. Tawfik and I. Mishustin, Journal of Physics G: Nuclear and Particle Physics **46**, 125201 (2019).
- [17] M. A. Stephanov, International Journal of Modern Physics A **20**, 4387 (2005).
- [18] F. Karsch, Journal of Physics G: Nuclear and Particle Physics **31**, S633 (2005).
- [19] P. Huovinen and P. Petreczky, Nucl. Phys. A **837**, 26 (2010).
- [20] S. Borsanyi et al., JHEP **09**, 073 (2010).
- [21] R. L. Workman and Others, PTEP **2022**, 083C01 (2022).
- [22] S. Samanta, S. Chatterjee, and B. Mohanty, Journal of Physics G: Nuclear and Particle Physics **46**, 065106 (2019).
- [23] V. Vovchenko et al., Physical Review C **96**, 045202 (2017).
- [24] A. Tawfik, Phys. Rev. D **71**, 054502 (2005).
- [25] P. Huovinen and P. Petreczky, Phys. Lett. B **777**, 125 (2018).
- [26] V. Vovchenko, A. Pasztor, Z. Fodor, S. D. Katz, and H. Stoecker, Phys. Lett. B **775**, 71 (2017).
- [27] V. Vovchenko, A. Motornenko, M. I. Gorenstein, and H. Stoecker, Phys. Rev. C **97**, 035202 (2018).
- [28] R. Dashen, S.-k. Ma, and H. J. Bernstein, Physical Review **187**, 345 (1969).
- [29] R. Venugopalan and M. Prakash, Nuclear Physics A **546**, 718 (1992).
- [30] P. M. Lo, The European Physical Journal C **77**, 533 (2017).
- [31] K. A. Olive, Nuclear Physics B **190**, 483 (1981).

- [32] K. A. Olive, Nuclear Physics B **198**, 461 (1982).
- [33] R. Hagedorn and J. Rafelski, Physics Letters B **97**, 136 (1980).
- [34] M. I. Gorenstein, V. Petrov, and G. Zinovjev, Physics Letters B **106**, 327 (1981).
- [35] R. Hagedorn, Zeitschrift für Physik C Particles and Fields **17**, 265 (1983).
- [36] J. I. Kapusta and K. A. Olive, Nucl. Phys. A **408**, 478 (1982).
- [37] D. H. Rischke, M. I. Gorenstein, H. Stoecker, and W. Greiner, Zeitschrift für Physik C Particles and Fields **51**, 485 (1991).
- [38] D. Anchishkin and E. Suhonen, Nuclear Physics A **586**, 734 (1995).
- [39] L. Satarov, M. Dmitriev, and I. Mishustin, Physics of Atomic Nuclei **72**, 1390 (2009).
- [40] A. Andronic, P. Braun-Munzinger, J. Stachel, and M. Winn, Physics Letters B **718**, 80 (2012).
- [41] A. Bhattacharyya, S. Das, S. K. Ghosh, R. Ray, and S. Samanta, Physical Review C **90**, 034909 (2014).
- [42] M. Albright, J. Kapusta, and C. Young, Physical Review C **90**, 024915 (2014).
- [43] V. Vovchenko, D. Anchishkin, and M. Gorenstein, Physical Review C **91**, 024905 (2015).
- [44] M. Albright, J. Kapusta, and C. Young, Physical Review C **92**, 044904 (2015).
- [45] K. Redlich and K. Zalewski, Physical Review C **93**, 014910 (2016).
- [46] P. Alba, W. M. Alberico, A. Nada, M. Panero, and H. Stöcker, Physical Review D **95**, 094511 (2017).
- [47] J. Cleymans, H. Oeschler, K. Redlich, and S. Wheaton, Physical Review C **73**, 034905 (2006).
- [48] V. Begun, M. Gaździcki, and M. Gorenstein, Physical Review C **88**, 024902 (2013).
- [49] J. Fu, Physics Letters B **722**, 144 (2013).
- [50] V. Vovchenko and H. Stoecker, Physical Review C **95**, 044904 (2017).
- [51] P. Alba, V. Vovchenko, M. Gorenstein, and H. Stoecker, Nuclear Physics A **974**, 22 (2018).
- [52] L. Satarov, V. Vovchenko, P. Alba, M. Gorenstein, and H. Stoecker, Physical Review C **95**, 024902 (2017).
- [53] V. Vovchenko, M. I. Gorenstein, and H. Stoecker, Physical review letters **118**, 182301 (2017).
- [54] P. Huovinen and P. Petreczky, Physics Letters B **777**, 125 (2018).
- [55] V. Vovchenko, Physical Review C **96**, 015206 (2017).
- [56] P. Braun-Munzinger and J. Stachel, arXiv preprint nucl-ex/9803015 (1998).
- [57] A. Tawfik, M. El-Bakry, D. Habashy, M. Mohamed, and E. Abbas, International Journal of Modern Physics E **25**, 1650018 (2016).
- [58] A. N. Tawfik, A. M. Diab, and M. Hussein, Journal of Physics G: Nuclear and Particle Physics **45**, 055008 (2018).
- [59] N. Kalmykov, S. Ostapchenko, and A. Pavlov, Nuclear Physics B-Proceedings Supplements **52**, 17 (1997).
- [60] N. Kalmykov and S. Ostapchenko, Physics of Atomic Nuclei **56**, 346 (1993).
- [61] S. Ostapchenko, Physical Review D **74**, 014026 (2006).
- [62] S. Ostapchenko, Nuclear Physics B-Proceedings Supplements **151**, 143 (2006).
- [63] S. Ostapchenko, Status of qgsjet, in *AIP Conference Proceedings*, volume 928, pages 118–125, American Institute of Physics, 2007.

- [64] J. Engel, T. Gaisser, P. Lipari, and T. Stanev, Physical Review D **46**, 5013 (1992).
- [65] R. Fletcher, T. Gaisser, P. Lipari, and T. Stanev, Physical Review D **50**, 5710 (1994).
- [66] E.-J. Ahn, R. Engel, T. K. Gaisser, P. Lipari, and T. Stanev, Physical Review D **80**, 094003 (2009).
- [67] K. Werner, F.-M. Liu, and T. Pierog, Physical Review C **74**, 044902 (2006).
- [68] T. Pierog and K. Werner, Nuclear Physics B-Proceedings Supplements **196**, 102 (2009).
- [69] M. Hanafy and M. Maher, (2020).
- [70] G. E. Uhlenbeck and E. Beth, Physica **3**, 729 (1936).
- [71] E. Beth and G. E. Uhlenbeck, Physica **4**, 915 (1937).
- [72] A. Kostyuk, M. Gorenstein, H. Stöcker, and W. Greiner, Physical Review C **63**, 044901 (2001).
- [73] V. Vovchenko, A. Motornenko, M. I. Gorenstein, and H. Stoecker, Physical Review C **97**, 035202 (2018).
- [74] K. Huang, New York (1963).
- [75] L. Landau, Course of Theoretical Physics **5**, 396 (1980).
- [76] W. Greiner, L. Neise, and H. Stöcker, *Thermodynamics and statistical mechanics*, Springer Science & Business Media, 2012.
- [77] G. Fast, R. Hagedorn, and L. Jones, Il Nuovo Cimento (1955-1965) **27**, 856 (1963).
- [78] G. Fast, Nuovo Cimento J **2**, 856 (1963).
- [79] R. Eden, P. Landshoff, and D. Olive, Polkinghorne jc å the analytic s-matrix, 1966.
- [80] F. Karsch, K. Redlich, and A. Tawfik, Eur. Phys. J. **C29**, 549 (2003).
- [81] F. Karsch, K. Redlich, and A. Tawfik, Phys. Lett. **B571**, 67 (2003).
- [82] K. Redlich, F. Karsch, and A. Tawfik, J. Phys. **G30**, S1271 (2004).
- [83] A. Tawfik and D. Toublan, Phys. Lett. B **623**, 48 (2005).
- [84] A. Tawfik and E. Abbas, Physics of Particles and Nuclei Letters **12**, 521 (2015).
- [85] T. Pierog, I. Karpenko, J. M. Katzy, E. Yatsenko, and K. Werner, Physical Review C **92**, 034906 (2015).
- [86] A. Bzdak et al., Phys. Rept. **853**, 1 (2020).
- [87] T. Anticic et al., Physical review letters **93**, 022302 (2004).
- [88] S. Afanasiev et al., Phys. Lett. B **358**, 275 (2002).
- [89] C. Alt et al., Physical review letters **94**, 192301 (2005).
- [90] S. Afanasiev et al., Physical Review C **66**, 054902 (2002).
- [91] C. Blume et al., Journal of Physics G: Nuclear and Particle Physics **31**, S685 (2005).
- [92] F. Antinori et al., Physics Letters B **595**, 68 (2004).
- [93] S. S. Adler et al., Phys. Rev. C **74**, 024904 (2006).
- [94] A. Taranenko, J. Phys. Conf. Ser. **1685**, 012021 (2020).
- [95] T. Galatyuk, Nucl. Phys. A **982**, 163 (2019).
- [96] J. Adam et al., Phys. Rev. C **93**, 034913 (2016).
- [97] M. A. Lisa et al., The E895 pion correlation analysis: A Status report, in *20th Winter Workshop on Nuclear Dynamics*, 2005.

[98] B. Back et al., Physical Review C **69**, 054901 (2004).